Tetrahydropyrazolo[1,5-*a*]pyridine-fused steroids and their in vitro biological evaluation in prostate cancer

Radek Jorda[1,#,*], Susana M. M. Lopes[2,#], Eva Řezníčková[1], Haresh Ajani[3], António V. Pereira[2], Clara S. B. Gomes[4], Teresa M. V. D. Pinho e Melo[2,*]

[1] Laboratory of Growth Regulators, The Czech Academy of Sciences, Institute of Experimental Botany & Palacký University, Šlechtitelů 27, 783 71 Olomouc, Czech Republic

[2] CQC and Department of Chemistry, University of Coimbra, 3004-535 Coimbra, Portugal

[3] Structural Genomics Consortium, University of Toronto, Toronto, ON M5G 1L7, Canada

[4] LAQV-REQUIMTE, Departamento de Química, Faculdade de Ciências e Tecnologia, Universidade NOVA de Lisboa, 2829-516, Caparica, Portugal

Corresponding Authors

*Corresponding author for biological part, E-mail: radek.jorda@upol.cz

*Corresponding author for chemistry part, E-mail: tmelo@ci.uc.pt

Author Contributions

The manuscript was written through contributions of all authors. All authors have given approval to the final version of the manuscript. #These authors contributed equally.

Keywords

galeterone, steroid, androgen, prostate, pyrazolo[1,5-*a*]pyridine

Abstract

The androgen receptor (AR) is a steroid hormone receptor and its high expression and disruption of its regulation are strongly implicated in prostate cancer (PCa) development. One of the current therapies includes application of steroidal antiandrogens leading to blockade of the AR action by the abrogation of AR-mediated signaling. We introduced here novel 4,5,6,7-tetrahydropyrazolo[1,5-*a*]pyridine-fused steroidal compounds, described their synthesis based on [8π+2π] cycloaddition reactions of diazafulvenium methides with different steroidal scaffolds and showed their biological evaluation in different prostate cancer cell lines *in vitro*. Our results showed the ability of novel compounds to suppress the expression of known androgen receptor targets, Nkx3.1 and PSA in two prostate cell lines, 22Rv1 and VCaP. Candidate compound diminished the transcription of AR-regulated genes in the reporter cell line in a concentration-dependent manner. Antiproliferative activity of the most promising steroid was studied by clonogenic assay and induction of apoptosis in treated cells was documented by immunoblot detection of cleaved PARP.

Graphical abstract

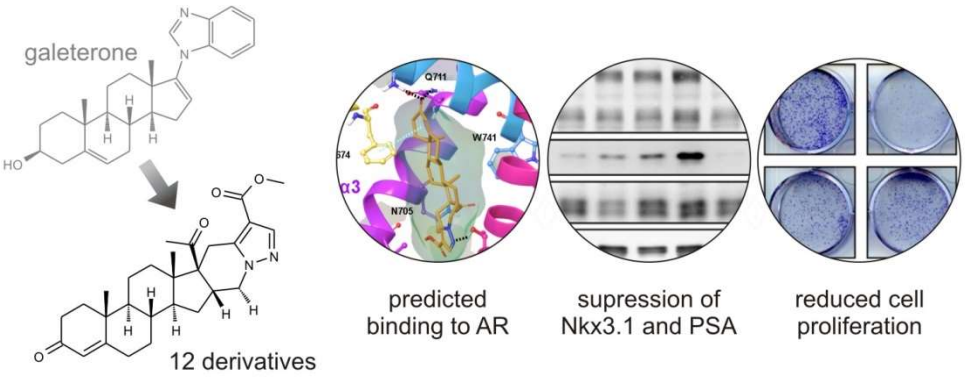

Introduction

Castration resistant prostate cancer (PCa) is one of the main causes of male cancer associated deaths worldwide and the blockade of androgen receptor (AR) action is considered as an effective way for the treatment. Reactivation of AR transcriptional activity via multiple mechanisms [1] represents a driving force for ongoing development of castration resistance. Current therapeutics include steroidal and nonsteroidal antiandrogens (**Figure 1**) targeting mostly ligand-binding domain of AR [2–5] although other modulators targeting another domains are rapidly investigated and exhibit beneficial preclinical profiles [1,6].

Among steroidal antiandrogens, galeterone is described as a multitargeted molecule that can antagonize AR, enhance the degradation of AR and its splice variants and inhibit AR nuclear translocation [7]. Furthermore, galeterone inhibits one of key enzymes in steroidal biosynthesis, 17α-hydroxylase/17,20-lyase (CYP17A1), and the targeting of two deubiquitinating enzymes USP12 and USP46 that control AR degradation has been recently described [8]. Unfortunately, galeterone's effectivity is attenuated by its metabolism, that revealed products with diverse biochemical activities [9]. Furthermore, the latest study from clinical trials in men with AR-V7-expressing CRPC tumors was abandoned due to insufficient response [1]. All these findings highlighted the need of further AR-interacting molecules for PCa treatment.

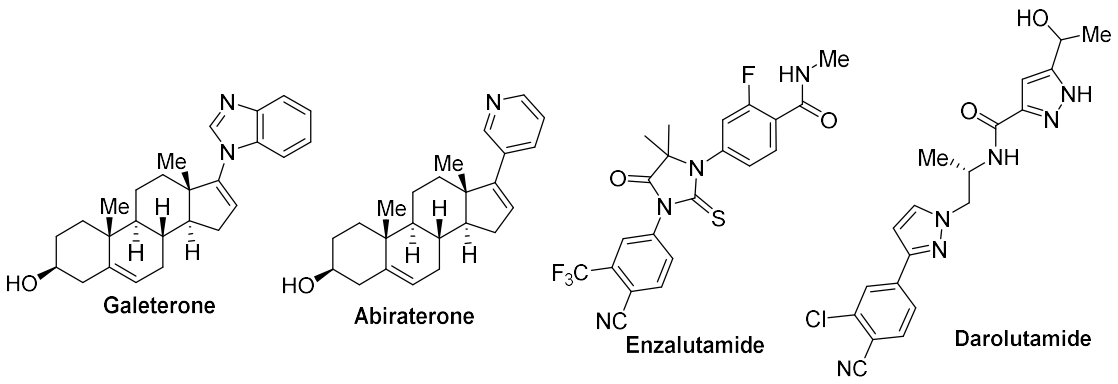

Figure 1. Examples of different types of antiandrogens from clinical trials of prostate cancer (source: clinicaltrials.gov)

Natural and synthetic steroids are an important class of compounds in which structural modifications of their basic core is largely used as a strategy to modulate biological properties [10–13]. In fact, the introduction of side chains/heterocycles or heterocycles fused at positions 16 and 17 of the D-ring led to steroids with interesting biological properties [13–15].

Successful examples of these transformations are galeterone and abiraterone, which contain a *N*-heterocycle at position C17 of the basic structure of steroid.

In this context, we have been interested in the synthetic modulations of the basic core of steroids, namely through [8π+2π] cycloaddition reactions of diazafulvenium methides with different steroidal scaffolds [16, 17] and by annulation reactions of a steroidal *N*-sulfonyl-1-azadiene with carbonyl compounds under enamine catalysis [18].

It was demonstrated that diazafulvenium methides **2**, generated *in situ* by the SO_2 extrusion of 2,2-dioxo-1*H*,3*H*-pyrazolo[1,5-*c*][1,3]thiazole **1**, react *via* [8π+2π] cycloaddition reaction with 16-dehydropregnenolone acetate (**16-DPA**), 16-dehydropregnenolone (**16-DHP**) or 16-dehydroprogesterone to produce chiral 4,5,6,7-tetrahydropyrazolo[1,5-*a*]pyridine-fused steroids in a regio- and stereoselective fashion (**Scheme 1**) [16, 17]. The first anticancer activity screening of these hexacyclic steroids showed that compounds containing a benzyl group at C-22, derived from **16-DHP** (**6**) and 16-dehydroprogesterone (**10**), show considerable cytotoxicity against EL4 (murine T-lymphoma) whereas the corresponding C-22 unsubstituted steroids show low cytotoxicity [17].

Herein, the biological evaluation in prostate cancer cell lines of hexacyclic steroids **4-11** whose synthesis has been previously described [16, 17], as well as new steroidal derivatives **12-15** is reported.

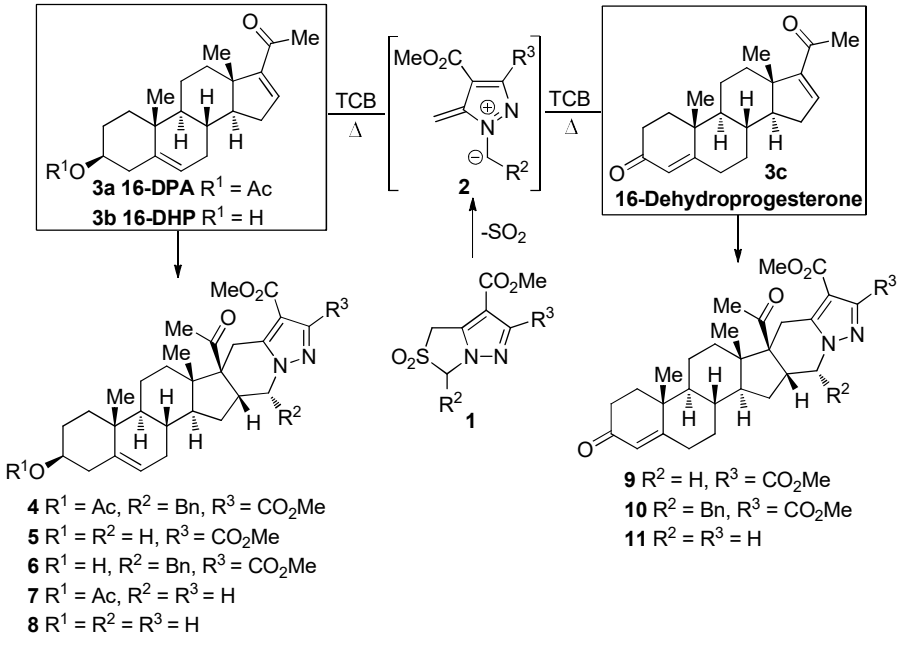

Scheme 1. Synthesis of chiral hexacyclic steroids by [8π+2π] cycloaddition reactions of diazafulvenium methides **2** with different steroidal scaffolds.

Results and discussion

Chemistry

Hexacyclic steroids **5**, **6** and **8** were synthetized by [8π+2π] cycloaddition reaction of diazafulvenium methides **2** with **16-DHP**, following the procedure described previously [17]. In order to modulate their hydrophilicity, steroids **5**, **6** and **8** were reduced to the corresponding hydroxymethyl derivatives (**Scheme 2**). Carrying out the reaction of steroid **5** with an excess of lithium aluminium hydride (3 equivalents per carbonyl group) in tetrahydrofuran at reflux, the expected hydroxymethyl derivative **12b** was obtained in 50% yield, together with the *O*-acetylated derivative **12a**, isolated in 21% yield (**Scheme 2**).

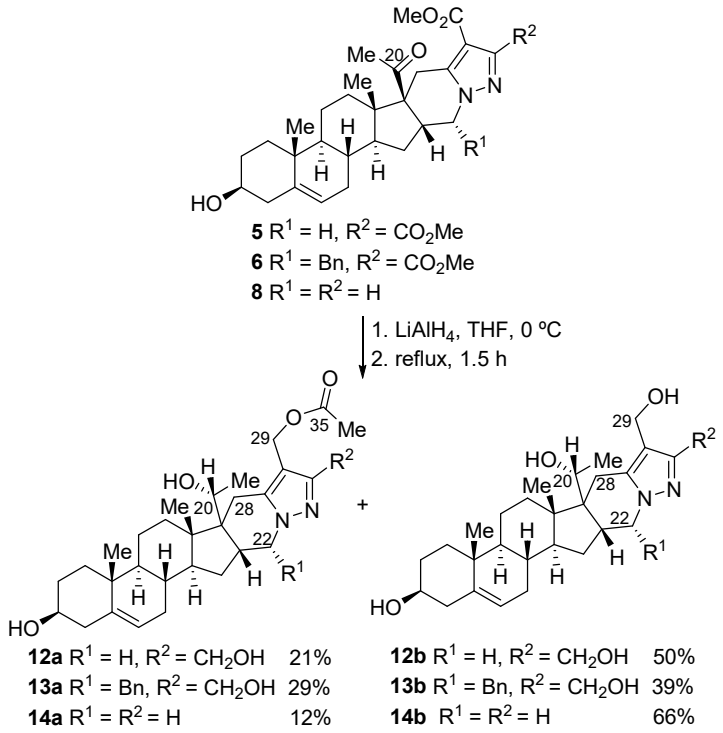

Scheme 2. Reduction of the steroid derivatives.

As expected, the acetyl substituent at C20 also underwent reduction to the corresponding alcohol along with the reduction of the two ester groups. Interestingly, the reduction of the acetyl group occurs diastereoselectively. Only one diastereoisomer was formed, whose molecular structure was unambiguously established by X-ray crystallography (**Figure 2**). This derivative crystallized as colourless needles in the orthorhombic system within $P2_12_12_1$ space group, showing one molecule *per* asymmetric unit. Its molecular structure consists of a steroid

derivative fused to 2,3-dihydroxymethyl-4,5,6,7-tetrahydropyrazolo[1,5-*a*]pyridine by the C16–C17 bond. Chiral centres C10, C13 and C3 retain the original configuration, whereas the newly formed chiral centres at positions C16, C17 and C20 display *R*, *S* and *R* configurations, respectively. All distances and angles are within the expected values for similar compounds [19].

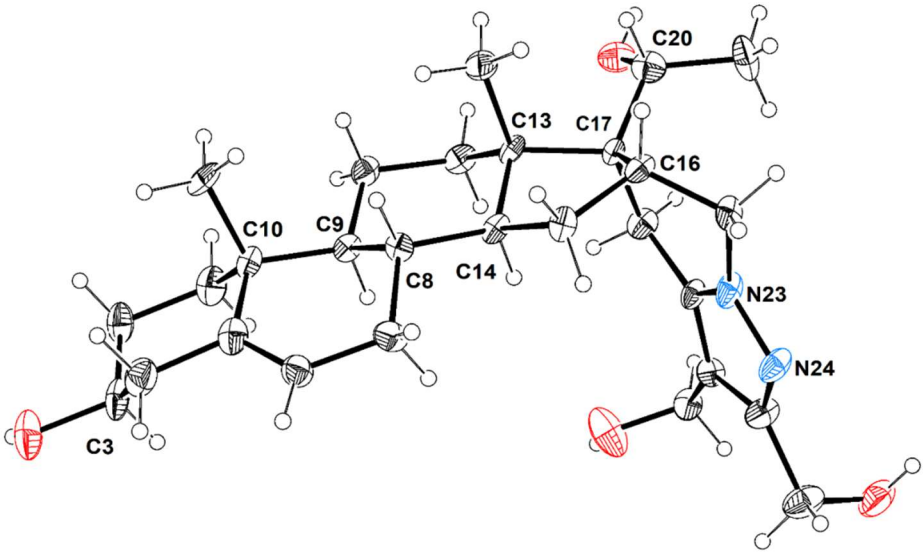

Figure 2. ORTEP-3 diagram of compound **12b**, using 30% probability level ellipsoids. Selected bond lengths (Å): C16−C17, 1.528(11); C17−C20, 1.535(11); C20−C21, 1.534(12); O33−C20, 1.432(11); N23−N24, 1.376(9); N23−C27, 1.308(9); N24−C25, 1.308(10); N23−C22, 1.447(10); C25−C26, 1.409(11); C26−C27, 1.378(11); Selected bond angles (º): C22–C16–C15 111.2(6); C16–C17–C20 112.3(7); C28–C17–C13, 110.8(6).

The acetyloxymethyl steroid derivative **12a** was formed by the reaction of **12b** with ethyl acetate which was added to destroy the unreacted lithium aluminium hydride before the isolation procedure. The presence of an acetyl group was easily identified in the ^{1}H NMR (δ_H = 2.03 ppm) and ^{13}C NMR (δ_C = 172.8 ppm) spectra of compound **12a**. The selective protection of one hydroxyl was confirmed based on two-dimensional spectra (see Supporting Information). Cross peaks were observed in the NOESY spectrum between protons H29 and protons H28, and the HMBC spectrum shows coupling between H29 and carbon C35. Moreover, the treatment of a methanol solution of compound **12a** with NaOH 2 M for 6 hours at room temperature, gave compound **12b** in quantitative yield (**Scheme 3**).

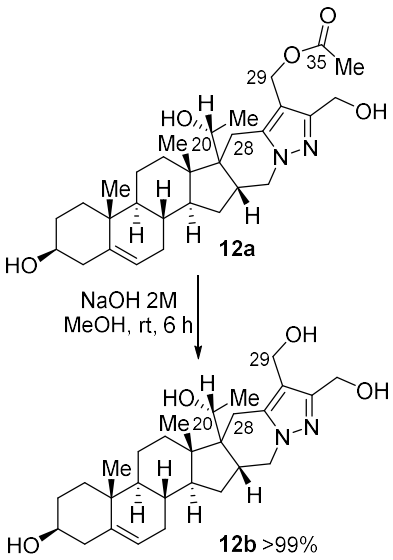

Scheme 3. Conversion of derivative **12a** into **12b**.

The reduction of the carbonyl groups of steroid **6**, which contain a benzyl group at C22, gave steroid **13b** in 39% yield, along with the formation of the acetyloxymethyl derivative **13a** in 29% yield. A similar reactivity was observed in the reduction of monocarboxylate steroid **8**, affording compounds **14a** (12%) and **14b** (66%) in 78% overall yield (**Scheme 2**).

Finally, the hydrolysis of the ester group of hexacyclic steroid **11** [17], prepared by [8π+2π] cycloaddition reaction of diazafulvenium methide **2** (R^2 = R^3 = H) with 16-dehydroprogesterone, was carried out using an aqueous potassium hydroxide solution in ethanol at room temperature for 2 hours. The acid derivative **15** was obtained in 55% yield (**Scheme 4**).

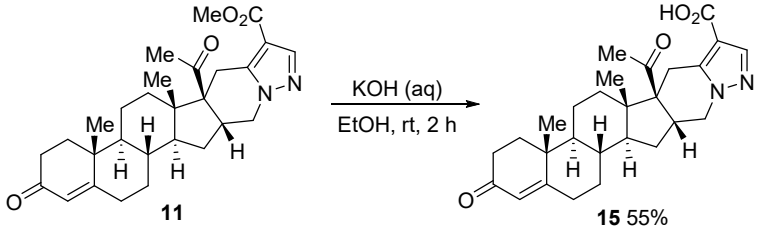

Scheme 4. Hydrolysis of steroid **11**.

Antiproliferative effect of studied compounds

All presented steroids were tested for their antiproliferative properties against five prostate cancer cell lines including androgen receptor positive vs negative cell lines and also

representatives of metastatic or CRPC cell lines; the resulting data are presented in **Table 1**. The results clearly show that most compounds do not reached measurable GI_{50} values (GI_{50} > 40 μM). Nevertheless, we evaluated residual viability in the presence of 40 μM compound that showed partial antiproliferative activities of the studied steroids (**Table 1**). Reduced viability in treated cells was almost comparable for all tested cell lines, only steroids' efficacy was significantly impaired in PC3 cell line. This trend is possibly linked with the absence androgen receptor in PC3 cells, that therefore become more resistant to the tested compounds as also documented for galeterone [20,21].

Table 1. Antiproliferative activities of novel steroids.

Steroids	Viability (40 μM)*				
	LNCaP	LAPC-4	PC-3	22Rv1 ARE14	VCaP
4	89.7	>100	>100	15.0	85.9
5	-	-	71.7	88.0	>100
6	83.5	81.3	64.7	28.4	57.0
7	-	-	>100	83.3	84.9
8	-	-	89.6	78.5	90.4
9	-	-	94.0	73.5	80.3
10	80.6	97.2	>100	63.3	80.7
11	77.3	95.1	98.3	80.4	85.1
12b	92.8	97.5	>100	95.8	96.3
13b	89.7	85.9	>100	55.8	43.0
14b	82.8	92.2	>100	96.3	96.7
15	-	-	>100	92.4	95.7
Galeterone	91.6	92.8	>100	25.14	57.2
Enzalutamide	94.2	80.3	>100	98.1	61.2

* viability in the presence of 40 μM compound (10 μM for galeterone), measured at least in triplicate.

The effect of steroids on the transcriptional activity of androgen receptor

Despite the fact that all studied steroids did not potently influence antiproliferative properties of examined PCa cell lines, we further investigated their influence on i) some AR-regulated genes via immunoblotting and ii) the transcriptional activity of androgen receptor using an AR-dependent reporter cell line, 22Rv1-ARE14 [22]. As shown in **Figure 2**, immunoblot analysis revealed that protein expression of known AR-targets, Nkx3.1 and PSA were decreased in the presence of some steroids compared to untreated cells, while the protein expression of androgen

receptor with its V7 variant did not changed markedly. The most significant downregulation of Nkx3.1 was observed for steroids **8** and **11** that was also comparable to the effect of standards galeterone and enzalutamide. Notably, some compounds (**7, 8, 10, 11** and **13b**) actively decreased the expression of PSA more than the used standard. Whereas the expression of PSA remained unchanged under the defined conditions, expression of the AR transcription target Nkx3.1 was suppressed upon treatment with some steroids (e.g. **9, 12b**) probably due to low stability of the Nkx3.1 protein [23]. Finally, steroids **4**-**6** and **15** did not affect any of both proteins.

Further, we compared the effects of the studied steroids (10 μM sub-lethal concentration, 24h treatment) on AR-transcriptional activity using 22Rv1-ARE14 cells in the presence of R1881. As shown in **Figure 2B**, most of the studied compounds did not abolish R1881-induced luciferase activity in 22Rv1-ARE14 cells. As expected, luciferase activity was blocked in the presence of antiandrogen enzalutamide and galeterone. Only steroid **11** markedly diminished the activity to 40% in comparison to R1881-stimulated control cells. This effect was comparable with the value obtained after the treatment of cells with antiandrogen galeterone.

Next, the activity of **11**, the most potent steroid compound in the series, was studied in more detail. To evaluate whether increasing treatment time would improve the relative antiproliferative effect of **11** we studied 22Rv1 colony development during 10 days. Our data (see **Figure 2C**) showed the ability of **11** to significantly inhibit colony formation in the studied cells.

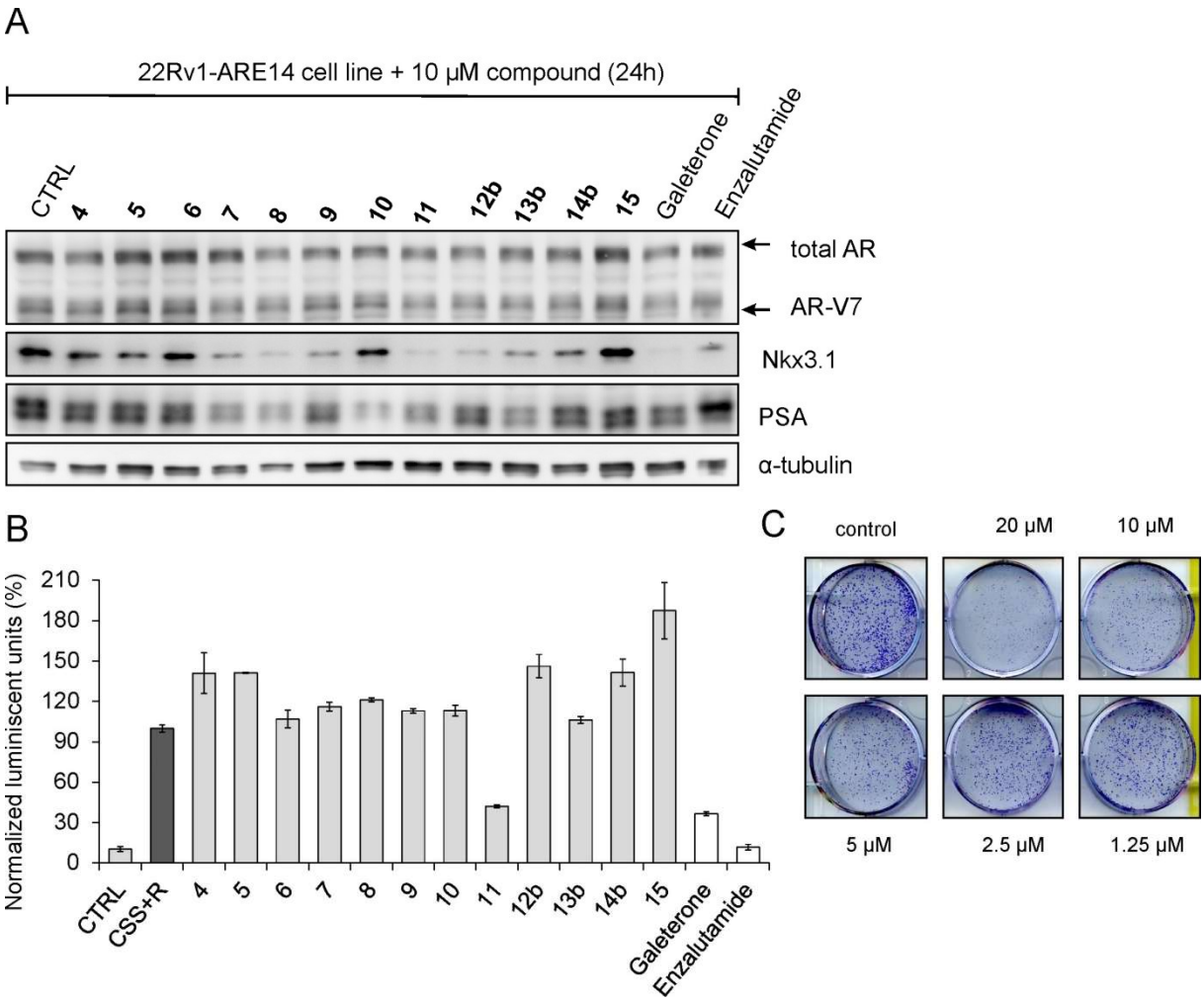

Figure 2. The influence of steroids derivatives on the AR-mediated transcription in the 22Rv1-ARE14 reporter cell line. (A) The cells were treated with the studied steroids (10 μM, 24 hours) and galeterone and enzalutamide (as a standard). Lysates were blotted for detection of appropriate proteins; α-tubulin was included as control for protein loading. (B) Cells were stimulated with 1 nM R1881 (R) alone (black column) or with different doses of steroids (10 μM, grey columns) for 24 h in charcoal-stripped serum medium (CSS), and then, the luciferase activity in the cell lysate was measured. Enzalutamide and galeterone were served as positive controls (white columns). (C) 22Rv1-ARE14 cells seeded in six-well plates were treated with indicated concentrations of **11** for 10 days; media were replaced once in 5th day.

Biological evaluation of steroidal compound 11

In the reporter cell line we showed that the treatment of 22Rv1-ARE14 cells with different concentrations of **11** reduced luciferase activity in a dose-dependent manner (**Figure 3A**). We further performed an immunoblotting analysis to monitor whether **11** can influence the expression of the known AR transcriptional targets in treated 22Rv1 cells. Our results showed

that steroid **11** decreased levels of both proteins in dose-dependent manner, which clearly correlated with the luciferase activity in these cells. Similar trends were observed after the treatment of cells with galeterone that showed to increase apoptosis more effectively than **11** as documented by stronger cleavage of PARP, a known caspase-3 substrate (see **Figure 3B**).

Immunoblotting analysis of AR-regulated proteins was also performed in VCaP cells (metastatic model of vertebral cancer of the prostate), but no significant changes in Nkx3.1 and PSA were observed upon 24 h treatment (**Figure 3C**). We only detected the cleaved PARP pointed at ingoing apoptosis which was weaker than in VCaP cells treated with galeterone. We therefore evaluated whether **11** is able to affect AR-target expression during the longer period. As documented in **Figure 3D**, protein expression of Nkx3.1 and PSA continuously decreased, which in the case of the expression of PSA was already detected after two days of treatment.

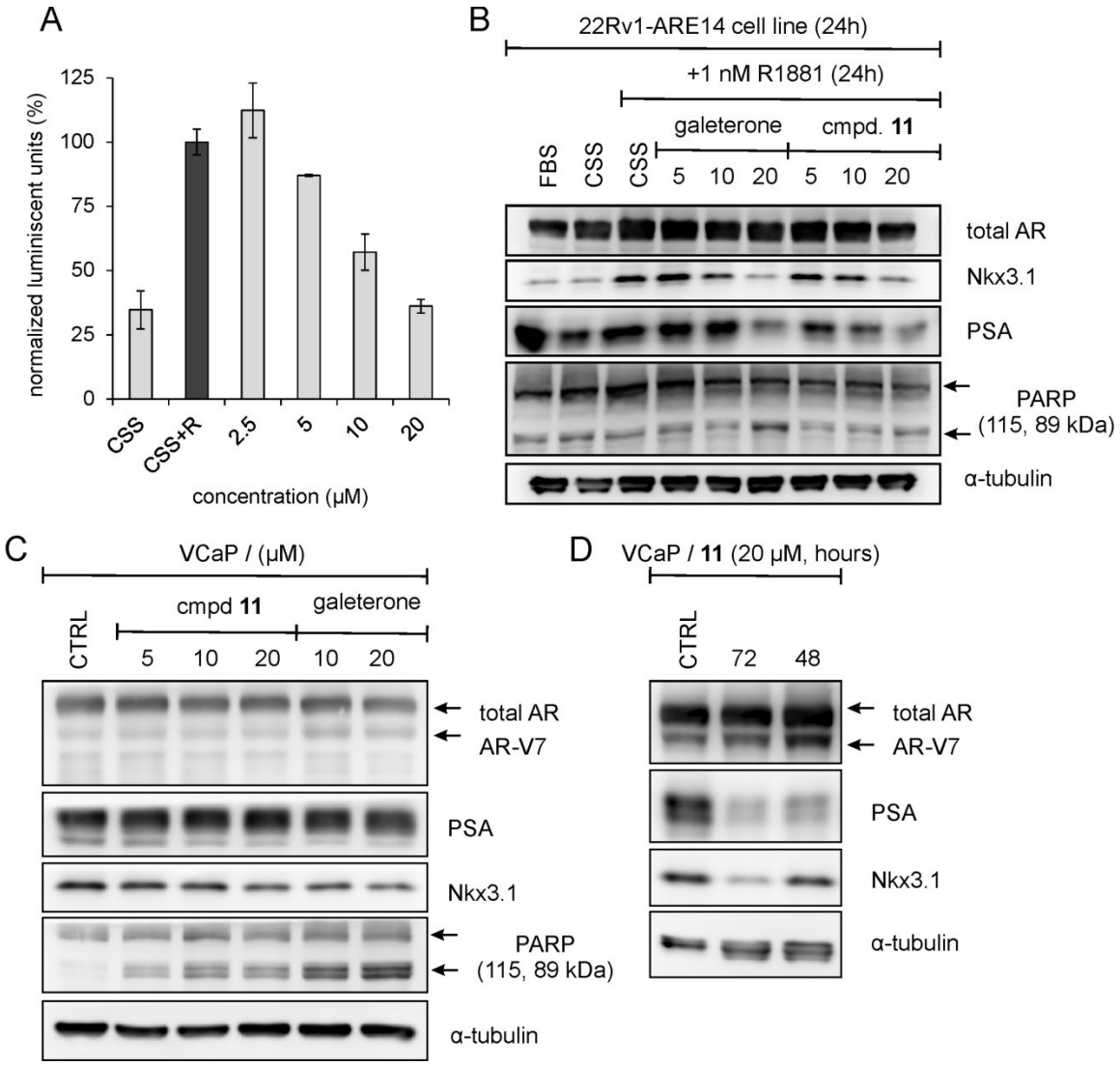

Figure 3. (A) The influence of steroid **11** on the AR-mediated transcription in the 22Rv1-ARE14 reporter cell line. Cells were stimulated with 1 nM R1881 (R) alone (black column) or

with different doses of **11** (grey columns) for 24 h in charcoal-stripped serum medium (CSS), and then, the luciferase activity in the cell lysate was measured. (B) The 22Rv1-ARE14 cells were cultivated in charcoal-stripped serum medium (CSS) for 24 h and then treated with different concentrations of **11** or galeterone (as a standard) in the presence of 1 nM R1881 for 24 hours. Lysates were blotted for detection of appropriate proteins. (C) The VCaP cells were treated with different concentrations of **11** or galeterone (as a standard) for 24 hours or (D) with 20 μM **11** for the indicated times and then lysates were blotted for detection of appropriate proteins. α-Tubulin was included as control for protein loading.

Binding mode of steroid 11 in the androgen receptor ligand binding domain

Protein flexibility plays an important role in determining receptor/ligand recognition. While critical to understanding receptor−ligand interactions, it is nontrivial to model these effects in the protein active site [24,25]. More than 70 ternary structures of AR available a human androgen receptor with a resolution < 2Å.

The binding modes of steroidal-core ligands revealed key elements to understand receptor flexibility and elucidate induced fit effects. AR structures have a 12 α-helices that define a central, mainly hydrophobic cavity where binding interactions are primarily guided by residues in helices 3, 5, 7,9, and 11 and in a β-strand located between helices 5 and 6 [26].

Induced fit docking of compound **11** into the AR ligand binding domain (PDB: 1T7T) reveals binding similar to galeterone and DHT. Key interaction in the AR structure, two residues (Arg752 and Gln711) located in the immediate vicinity of α9 of the steroid ligand are the most likely to create an interaction with the carboxyl group (**Figure 4A**). However, because of its strong positive charge, Arg752 is likely to be the one able to establish the strongest interaction with the ketone group. The position of its side chain is perfectly conserved in the AR structure in the complex with the three ligands studied, thus suggesting that it is particularly important for the binding of androgens by this receptor. At the other extremity of the steroid nucleus, Thr877 is well positioned for contacting the carboxyl group and for maintaining the steroid firmly inside the LBP (**Figure 4B**). The tetrahydropyrazolo ring of compound **11** makes hydrophobic contact with several hydrophobic residues.

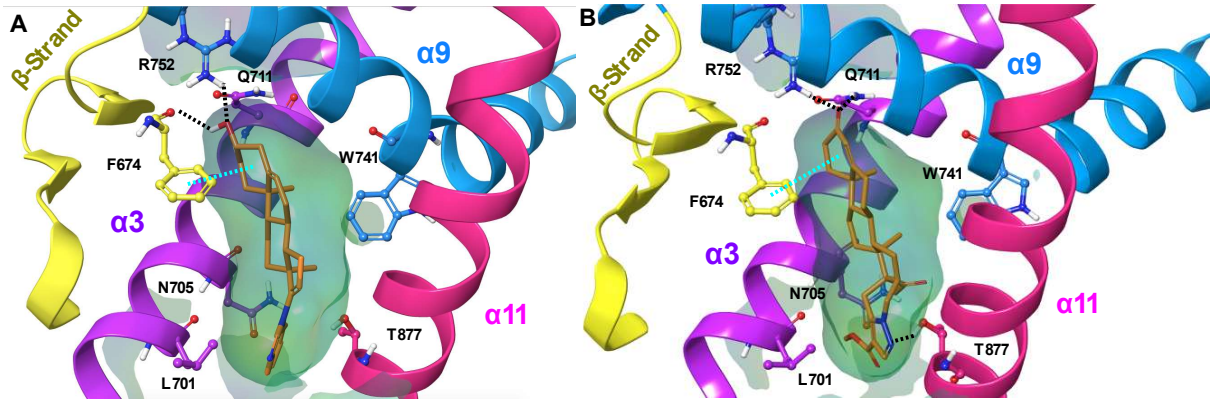

Figure 4. Docking complex proposed by IFD (flexible docking) for galeterone (A) and compound **11** (B) in AR (PDB: 1T7T). In all cases, ligands are shown with orange carbons, stick rendering; residues facing binding pocket are shown in ball-and-stick rendering; H-bond: black dashed line; stacking interaction: blue dashed line; helixes α3: magenta; α9: cyan; α11: pink; β-strand: yellow

Conclusion

In this article we evaluated twelve tetrahydropyrazolo[1,5-*a*]pyridine-fused steroids in several prostate cancer models. We showed their ability to suppress expression of known androgen receptor targets, Nkx3.1 and PSA, respectively. The candidate compound diminished transcription of AR-regulated genes in the reporter cell line in a concentration-dependent manner and also downregulated PSA and Nkx3.1 in two prostate cell lines. Finally, we showed that our candidate inhibits colony formation and induces apoptosis during the PCa treatment. Our results will contribute to finding further, effective steroidal antiandrogens for the treatment of CRPC.

Experimental

Chemistry

General. ^{1}H NMR spectra were recorded on an instrument operating at 400 MHz. ^{13}C NMR spectra were recorded on an instrument operating at 100 MHz. The solvent was tetradeuteromethanol unless otherwise indicated. Chemical shifts are expressed in parts per million relative to internal TMS, and coupling constants (*J*) are in Hz. Infrared spectra (IR) were recorded on a Fourier transform spectrometer. High-resolution mass spectra (HRMS) were obtained on an electrospray (ESI) TOF mass spectrometer. Melting points were determined in open glass capillaries and are uncorrected. Optical rotations were measured on an Optical Activity AA-5 electrical polarimeter. Thin-layer chromatography (TLC) analyses were

performed using precoated silica gel plates. Flash column chromatography was performed with silica gel 60 as the stationary phase.

*General procedure for the synthesis of hydroxyl steroid derivatives **12**, **13** and **14***. A solution of appropriate hexacyclic steroid **5**, **6** or 8［17］(0.20 mmol) in dry tetrahydrofuran (6 mL) was added dropwise to a suspension of lithium aluminium hydride (1.8 mmol for **5** and **6**, 1.2 mmol for **8**) in dry tetrahydrofuran (9 mL) at 0 ºC. The reaction mixture was stirred at this temperature for 15 minutes and then at reflux for 1.5 hours. The excess of lithium aluminium hydride was carefully decomposed by the addition of ethyl acetate followed by slow addition of water (0.1 mL), NaOH 15% (0.1 mL) and water (0.3 mL). The mixture was kept stirring for 1 hour. After this time, the mixture was filtered through celite and the inorganic residue washed with several portions of hot ethyl acetate. The filtrate was dried (Na_2SO_4) and the solvent evaporated off. The crude product was purified by flash chromatography.

3-Acetyloxymethyl-2-hydroxymethyl-4,5,6,7-tetrahydropyrazolo[1,5-*a*]pyridine fused to 20β-hydroxypregnenolone (**12a**) and **2,3-Dihydroxymethyl-4,5,6,7-tetrahydropyrazolo[1,5-*a*]pyridine fused to 20β-hydroxypregnenolone** (**12b**): Obtained from steroid **5** (105 mg, 0.20 mmol). Purification of the crude product by flash chromatography [ethyl acetate/methanol (95:5)] gave, in order of elution, **12a** as a white solid (20.7 mg, 21%) and **12b** as a white solid (47 mg, 50%).

Compound 12a: mp > 120 ºC (with decomposition) (from diethyl ether). $[\alpha]_D^{25}$ -60 (*c* 0.5 in MeOH). IR (ATR) ν 1016, 1226, 1376, 1457, 1734, 2931 and 3342 cm^{-1}. ^1H NMR δ: 0.79-0.89 (m, 2H), 1.03 (s, 3H), 1.05 (s, 3H), 1.16 (d, *J* = 6.4 Hz, 3H), 1.18-1.20 (m, 2H), 143-1.60 (m, 4H), 1.64-1.96 (m, 7H), 2.03 (s, 3H), 2.18-2.23 (m, 2H), 2.45-2.49 (m, 1H), 2.75 (d, *J* = 17.6 Hz, 1H), 3.12 (d, *J* = 17.6 Hz, 1H), 3.34-3.40 (m, 1H), 3.99 (dd, *J* = 13.2 and 3.2 Hz, 1H), 4.06 (dd, *J* = 13.2 and 4.0 Hz, 1H), 4.24 (q, *J* = 6.4 Hz, 1H), 4.59 (d, *J* = 12.4 Hz, 1H), 4.65 (d, *J* = 12.4 Hz, 1H), 5.12 (d, *J* = 12.8 Hz, 1H), 5.16 (d, *J* = 12.8 Hz, 1H), 5.27 (br d, *J* = 4.8 Hz, 1H). ^{13}C NMR δ: 16.5, 19.8, 20.1, 20.8, 21.2, 22.0, 32.3, 33.3, 33.5, 34.6, 35.2, 37.7, 38.5, 40.6, 43.0, 50.1, 51.1, 52.2, 52.8, 54.8, 57.1, 57.4, 72.4, 72.7, 110.5, 122.2, 142.3, 143.8, 151.5, 172.8. HRMS (ESI-TOF) m/z for $C_{30}H_{45}N_2O_5$ $[M+H]^+$ calcd 513.3323, found 513.3324.

Compound 12b: mp > 250 ºC (with decomposition) (from diethyl ether). $[\alpha]_D^{25}$ -50 (*c* 0.5 in MeOH). IR (ATR) ν 1010, 1060, 1373, 1458, 2928, 3228 cm^{-1}. ^1H NMR δ: 0.82-0.95 (m, 2H),

1.03 (s, 3H), 1.05 (s, 3H), 1.13 (d, *J* = 6.4 Hz, 3H), 1.22-1.32 (m, 2H), 1.42-1.96 (m, 11H), 2.18-2.23 (m, 2H), 2.44-2.48 (m, 1H), 2.80 (d, *J* = 17.2 Hz, 1H), 3.06 (d, *J* = 17.2 Hz, 1H), 3.36-3.41 (m, 1H), 3.96 (dd, *J* = 13.2 and 3.2 Hz, 1H), 4.08 (dd, *J* = 13.2 and 4.4 Hz, 1H), 4.22 (q, *J* = 6.4 Hz, 1H), 4.59 (br s, 2H), 4.62 (s, 2H), 5.27 (br d, *J* = 4.4 Hz, 1H). ^{13}C NMR δ: 16.3, 19.8, 20.3, 20.7, 22.0, 32.3, 33.1, 33.5, 34.7, 35.3, 37.6, 38.5, 40.4, 43.0, 50.0, 51.1, 52.1, 52.6, 54.3, 54.6, 57.4, 72.4, 72.8, 115.2, 122.3, 142.2, 142.6, 150.9. HRMS (ESI-TOF) m/z for $C_{28}H_{43}N_2O_4$ $[M+H]^+$ calcd 471.3217, found 471.3208.

(7*S*)-3-Acetyloxymethyl-7-benzyl-2-hydroxymethyl-4,5,6,7-tetrahydropyrazolo[1,5-*a*]pyridine fused to 20β-hydroxypregnenolone (**13a**) and **(7*S*)-2,3-Dihydroxymethyl-7-benzyl-4,5,6,7-tetrahydropyrazolo[1,5-*a*]pyridine fused to 20β-hydroxypregnenolone** (**13b**): Obtained from steroid **6** (124 mg, 0.20 mmol). Purification of the crude product by flash chromatography [ethyl acetate/methanol (95:5)] gave, in order of elution, **13a** as a white solid (34.8 mg, 29%) and **13b** as a white solid (43.8 mg, 39%).

Compound 13a: mp > 160 ºC (with decomposition) (from diethyl ether). $[\alpha]_D^{25}$ -70 (*c* 0.5 in MeOH). IR (ATR) ν 1018, 1044, 1231, 1375, 1455, 1716, 2930 and 3361 cm^{-1}. ^{1}H NMR δ: 0.71-0.82 (m, 1H), 0.88 (s, 3H), 1.01 (s, 3H), 1.03 (d, *J* = 6.4 Hz, 3H), 1.07-1.20 (m, 2H), 1.28-1.32 (m, 2H), 1.36-1.73 (m, 7H), 1.77-1.93 (m, 4H), 2.01 (s, 3H), 2.13-2.24 (m, 2H), 2.56-2.65 (m, 1H), 2.96-3.07 (m, 1H), 3.25 (dd, *J* = 16.8 and 4.0 Hz, 1H), 3.36-3.40 (m, 1H), 3.78-3.87 (m, 1H), 4.05 (q, *J* = 6.4 Hz, 1H), 4.31-4.36 (m, 1H), 4.57-4.73 (m, 2H), 5.14-5.21 (m, 2H), 5.24-5.27 (m, 1H), 7.26-7.31 (m, 3H), 7.34-7.38 (m, 2H). ^{13}C NMR δ: 16.9, 19.5, 19.7, 20.9, 21.3, 22.0, 28.3, 32.3, 33.4, 33.6, 35.4, 36.7, 37.7, 38.5, 42.9, 43.9, 51.0, 52.8, 55.8, 56.1, 57.3, 57.5, 61.3, 72.4, 110.4, 122.3, 127.8, 129.8, 130.4, 139.0, 142.3, 144.3, 151.3, 172.8. HRMS (ESI-TOF) m/z for $C_{37}H_{51}N_2O_5$ $[M+H]^+$ calcd 603.3792, found 603.3771.

Compound 13b: mp > 190 ºC (with decomposition) (from diethyl ether). $[\alpha]_D^{25}$ -100 (*c* 0.5 in MeOH). IR (ATR) ν 1002, 1043, 1376, 1454, 2928 and 3311 cm^{-1}. ^{1}H NMR δ: 0.50-0.58 (m, 1H), 0.72-0.80 (m, 1H), 0.85 (s, 3H), 0.98 (s, 3H), 1.01 (d, *J* = 6.4 Hz, 3H), 1.05-1.16 (m, 2H), 1.25-1.58 (m, 6H), 1.64-1.96 (m, 6H), 2.15-2.18 (m, 2H), 2.58 (d, *J* = 17.2 Hz, 1H), 2.99 (dd, *J* = 13.2 and 11.2 Hz, 1H). 3.23 (d, *J* = 17.2 Hz, 1H), 3.33-3.38 (m, 1H), 3.18 (dd, *J* = 13.2 and 4.4 Hz, 1H), 4.02 (q, *J* = 6.4 Hz, 1H), 4.28-4.32 (m, 1H), 4.57 (d, *J* = 12.4 Hz, 1H), 4.62 (d, *J* = 12.4 Hz, 1H), 4.66 (s, 2H), 5.23 (br d, *J* = 4.4 Hz, 1H), 7.24-7.28 (m, 3H), 7.32-7.36 (m, 2H). ^{13}C NMR δ: 16.8, 19.6, 19.8, 20.8, 22.1, 28.2, 32.3, 33.1, 33.6, 35.6, 36.7, 37.5, 38.4, 43.0,

44.0, 49.6, 51.0, 52.7, 54.5, 55.8, 57.5, 61.3, 72.4, 72.5, 115.1, 122.3, 127.8, 129.7, 130.3, 139.1, 142.0, 143.2, 150.6. HRMS (ESI-TOF) m/z for $C_{35}H_{49}N_2O_4$ $[M+H]^+$ calcd 561.3687, found 561.3678.

3-Acetyloxymethyl-4,5,6,7-tetrahydropyrazolo[1,5-*a*]pyridine fused to 20β-hydroxypregnenolone (**14a**) and **3-Hydroxymethyl-4,5,6,7-tetrahydropyrazolo[1,5-*a*]pyridine fused to 20β-hydroxypregnenolone** (**14b**): Obtained from steroid **8** (93.3 mg, 0.20 mmol). Purification of the crude product by flash chromatography [ethyl acetate/methanol (95:5)] gave, in order of elution, **14a** as a white solid (11.5 mg, 12%) and **14b** as a white solid (58.2 mg, 66%).

Compound 14a: mp > 87.0 °C (with decomposition) (from diethyl ether). $[\alpha]_D^{25}$ -50 (*c* 0.5 in MeOH). IR (ATR) ν 1018, 1043, 1227, 1376, 1458, 1735, 2924 and 3345 cm^{-1}. ^1H NMR δ: 0.68-0.75 (m, 1H), 0.78-0.85 (m, 1H), 1.01 (s, 3H), 1.02 (s, 3H), 1.10-1.15 (m, 1H), 1.17 (d, *J* = 6.4 Hz, 3H), 1.18-1.20 (m, 1H), 1.41-1.70 (m, 9H), 1.88-1.95 (m, 2H), 2.00 (s, 3H), 2.16-2.19 (m, 2H), 2.72 (d, *J* = 17.2 Hz, 1H), 3.13 (d, *J* = 17.2 Hz, 1H), 3.34-3.38 (m, 1H), 4.01 (dd, *J* = 13.6 and 3.2 Hz, 1H), 4.06 (dd, *J* = 11.6 and 4.0 Hz, 1H), 4.24 (q, *J* = 6.4 Hz, 1H), 5.03 (s, 2H), 5.24 (br d, *J* = 4.8 Hz, 1H), 7.42 (s, 1H). ^{13}C NMR δ: 16.5, 19.8, 19.9, 20.7, 21.2, 22.0, 32.2, 33.3, 33.4, 34.5, 35.3, 37.6, 38.5, 40.9, 42.9, 50.1, 51.1, 52.5, 53.0, 55.1, 57.7, 72.4, 72.7, 112.5, 122.1, 141.1, 142.3, 142.7, 172.7. HRMS (ESI-TOF) m/z for $C_{29}H_{43}N_2O_4$ $[M+H]^+$ calcd 483.3217, found 483.3220.

Compound 14b: mp > 218 ºC (with decomposition) (from diethyl ether). $[\alpha]_D^{25}$ -40 (*c* 0.5 in MeOH). IR (ATR) ν 999, 1050, 1354, 1376, 1420, 2930 and 3276 cm^{-1}. ^1H NMR δ: 0.77-0.84 (m, 2H), 1.01 (s, 3H), 1.03 (s, 3H), 1.07-1.08 (m, 1H), 1.12 (d, *J* = 6.4 Hz, 3H), 1.18-1.25 (m, 2H), 1.47-1.52 (m, 4H), 1.62-1.69 (m, 2H), 1.76-1.86 (m, 3H), 1.91-1.94 (m, 1H), 2.16-2.19 (m, 2H), 2.43-2.45 (m, 1H), 2.78 (d, *J* = 17.2 Hz, 1H), 3.07 (d, *J* = 17.2 Hz, 1H), 3.35-3.40 (m, 1H), 3.98 (dd, *J* = 13.2 and 3.2 Hz, 1H), 4.08 (dd, *J* = 13.2 and 4.4 Hz, 1H), 4.21 (q, *J* = 6.4 Hz, 1H), 4.51 (s, 2H), 5.24 (br d, *J* = 0.4 Hz, 1H), 7.37 (s, 1H). ^{13}C NMR δ: 16.3, 19.8, 20.2, 20.6, 22.1, 32.3, 33.2, 33.4, 34.7, 35.4, 37.6, 38.5, 40.7, 43.0, 50.0, 51.2, 52.4, 52.7, 54.9, 55.2, 72.4, 72.8, 117.3, 122.2, 139.0, 141.4, 142.2. HRMS (ESI-TOF) m/z for $C_{27}H_{41}N_2O_3$ $[M+H]^+$ calcd 441.3112, found 441.3106.

*Procedure for conversion of **12a** into **12b**:*

Aqueous solution of NaOH 1M (0.3 mL) was added to a solution of compound **12a** (20 mg, 0.039 mmol) in methanol (3 mL). The mixture was stirried at room temperature for 6 hours. After this time, H_2O (10 mL) was added and the mixture extracted with ethyl acetate (3 x 10 mL). The organic extracts were dried (Na_2SO_4) and the solvent evaporated off. Compound **12b** was obtained as a white solid (18.3 mg, 99%) and was identified by comparison with the specimen previously isolated (see above).

4,5,6,7-Tetrahydropyrazolo[1,5-*a*]pyridine-3-carboxylic acid fused to progesterone, (**15**): A solution of compound **11** (41 mg, 0.0883 mmol) in ethanol (3 mL) was treated with a KOH saturated solution at room temperature for 2 h. After the reaction was complete (TLC control), the mixture was acidified with HCl 1M and extracted with ethyl acetate (3 x 15 mL). The organic phase was dried (Na_2SO_4) and the solvent evaporated off. Purification of the crude product by flash chromatography [chloroform/methanol (90:10)] gave compound **15** as a white solid (21.8 mg, 55%): mp >215 °C (with decomposition) (from diethyl ether). $[\alpha]_D^{25}$ +20 (*c* 0.5 in $CHCl_3$). IR (ATR) ν 1199, 1223, 1248, 1560, 1655, 1686, 1693 and 2939 cm^{-1}. ^1H NMR ($CDCl_3$) δ: 0.81 (s, 3H), 1.16 (s, 3H), 1.31-1.37 (m, 3H), 1.52-1.73 (m, 3H), 1.84-2.07 (m, 7H), 2.13-2.18 (m, 1H), 2.23 (s, 3H), 2.47-2.64 (m, 3H), 3.31 (d, *J* = 16.4 Hz, 1H), 3.43 (d, *J* = 16.4 Hz, 1H), 3.71-3.77 (m, 1H), 3.89 (dd, *J* = 13.2 and 6.4 Hz, 1H), 4.30 (dd, *J* = 13.2 and 6.4 Hz, 1H), 6.18 (s, 1H), 7.86 (s, 1H). ^{13}C NMR ($CDCl_3$) δ: 16.7, 17.6, 20.5, 24.7, 27.7, 30.8, 32.7, 33.8, 33.9, 35.4, 36.4, 39.4, 46.2, 46.3, 50.1, 51.0, 52.3, 66.1, 109.3, 126.0, 141.2, 142.7, 159.9, 167.9, 199.1, 200.8, 207.3. HRMS (ESI-TOF) m/z for $C_{27}H_{35}N_2O_4$ $[M+H]^+$ calcd 451.2591, found 451.2583.

Crystallographic data for 2,3-dihydroxymethyl-4,5,6,7-tetrahydropyrazolo[1,5-*a*]pyridine fused to 20β-hydroxypregnenolone (12b) X-ray diffraction. Crystals suitable for single-crystal X-ray analysis of compound **12b** were selected and covered with Fomblin (polyfluoro ether oil) and mounted on a nylon loop. The data was collected at room temperature on a Bruker D8 Venture diffractometer equipped with a Photon 100 detector and an Oxford Cryosystem Cooler, using graphite monochromated Mo-Kα radiation (λ = 0.71073 Å). The data was processed using the APEX3 suite software package, which includes integration and scaling (SAINT), absorption corrections (SADABS) and space group determination (XPREP). Structure solution and refinement were done using direct methods with the programs SHELXT 2014/5 and SHELXL (version 2018/3) [27,28] inbuilt in APEX and WinGX-Version 2018.3 [29] software packages. Despite the crystal of compound **12b** showing poor diffracting power,

and crystal quality (R_{int} of 0.2144), the structure refined to a good convergence. All non-hydrogen atoms were refined anisotropically. Hydrogen atoms were inserted in idealized positions, and allowed to refine riding on the parent carbon or oxygen atom with C–H distances of 0.93 Å, 0.96 Å, 0.97 Å, and 0.98 Å for aromatic, methyl, methylene and methine H atoms, respectively, and O–H distance of 0.82 Å. The molecular diagrams were drawn with ORTEP-3 (version 2014.1)[27,28], included in the software package. The data for **12b** was deposited in the CCDC under deposit number CCDC 1909726.

Experimental section

Cell lines

LNCaP cells were purchased from ECACC. LAPC-4 and VCaP were kindly provided by Dr. Frederic R. Santer from Innsbruck Medical University (Austria). The 22Rv1-ARE14 reporter cell line[22] was a generous gift from Prof. Zdeněk Dvořák (Department of Cell Biology and Genetics, Palacký University). The VCaP and LNCaP cell lines were grown in 25 mM HEPES-modified RPMI-1640 medium, The LAPC-4 cell line was grown in Iscove´s Modified Dulbecco´s medium, and the 22Rv1-ARE14 cell line was grown in RPMI-1640 medium. All media were supplemented with 10 % normal or charcoal-stripped fetal bovine serum, 4 mM glutamine, 100 IU/ml penicillin, 100 µg/ml streptomycin and 1 mM sodium pyruvate. Cells were maintained in a humidified CO_2 incubator at 37 °C.

Chemicals

Specific reagents were purchased from PerkinElmer (R1881) and Merck (galeterone). Enzalutamide was kindly provided by Dr. Frederic R. Santer from Innsbruck Medical University.

AR-transcriptional reporter assay

22Rv1-ARE14 cells were seeded into a 96-well plate. The next day, the cultivation medium was discarded and the cells were incubated in the absence or presence of the tested compounds dissolved in RPMI-1640 medium supplemented with charcoal-stripped serum and 1 nM R1881 for 7 hours. After an incubation period, the cells were washed with PBS and lysed for 10 min in a lysis buffer (10 mM Tris pH = 7.4, 2 mM DCTA, 1 % nonidet P40, 2 mM DTT). After lysing, a reaction buffer (20 mM tricin pH = 7.8, 1.07 mM $MgSO_4$. $7H_20$, 5 mM ATP, 9.4 µM luciferine) was added to the wells and the luminescence of the samples was measured using a Tecan M200Pro microplate reader (Biotek).

Cell viability assays

For the cytotoxicity assays, cells were treated in triplicate with six different doses of each compound for 72 h. After treatment, the resazurin (Merck) solution was added for 4 h, and then the fluorescence of resorufin was measured at 544 nm / 590 nm (excitation / emission) using a Fluoroskan Ascent microplate reader (Labsystems). The GI_{50} value, the drug concentration lethal to 50% of the cells, was calculated from the dose response curves that resulted from the assays.

Immunoblotting

Cell lysates were prepared, and then proteins were separated on SDS-polyacrylamide gels and electroblotted onto nitrocellulose membranes. After blocking, overnight incubation with specific primary antibodies, and incubation with peroxidase-conjugated secondary antibodies, peroxidase activity was detected with SuperSignal West Pico reagents (Thermo Scientific) using a CCD camera LAS-4000 (Fujifilm). The following specific antibodies were purchased from Cell Signaling Technology (anti-PARP, clone 46D11; anti-androgen receptor, clone D6F11; anti-PSA/KLK3, clone D6B1; anti-NKX3.1, clone D2Y1A; peroxidase conjugated secondary antibodies) and Merck (anti-α-tubulin, clone DM1A). All primary antibodies were diluted in TBS containing 3% BSA; 0.1% Tween 20.

22Rv1-ARE14 colony formation assay

2000 cells per well were seeded into 6-well plates. The following day the medium was removed and replaced with fresh medium containing different concentration of compound. Media containing compounds were replaced on the 5^{th} day. Then, medium was discarded and colonies were fixed with 70% ethanol for 15 min, washed with PBS and stained by crystal violet (1% solution in 96% ethanol) for 1 hour. Finally, plates were distained until the colonies were visible and digitized by camera.

Induced-fit (Flexible) Docking

All ligands were prepared using LigPrep and were optimized with the OPLS3 force field in the MacroModel module in Schrödinger [30−32]. The protein structure of 1T7T was applied with the flexible docking refinement method in the ICM. The correct atom types were assigned according to a modified version of ECEPP/3 force field [33]. Hydrogen atoms and missing heavy atoms were added. Tautomeric states of histidines and the positions of asparagine and

glutamine side chain amide groups were optimized to improve the hydrogen bond pattern. The cognate ligands were deleted from the complexes only after hydrogen optimization. The ICMPocketFinder function was used to identify the binding pocket in the crystal structures of Androgen receptor. The algorithm builds a grid map of a binding potential, and the position and size of the ligand-binding pocket are determined based on the construction of equipotential surfaces along those maps [34]. We applied the flexible ligand and receptor complex refinement implemented in ICM-Pro, followed by a global optimization of the flexible ligand in the receptor field, so that both the intramolecular ligand energy and the ligand–receptor interaction energy were optimized during the calculation.

Author Contributions

# these authors contributed equally; S.M.M.L. and A.V.P. prepared and characterized compounds, C.S.B.G performed the x-ray crystallography, H.A. provided molecular docking analysis, R.J. and E.Ř. performed biochemical and cellular experiments and analysed data, R.J., S.M.M.L. and T.M.V.D.P.eM. drafted the manuscript.

ORCID

Radek Jorda: 0000-0002-4905-7126
Susana M. M. Lopes: 0000-0002-1580-5667
Eva Řezníčková: 0000-0003-4773-2850
António V. Pereira: 0000-0002-5082-8688
Clara S. B. Gomes: 0000-0003-3672-0045
Teresa M. V. D. Pinho e Melo: 0000-0003-3256-4954
Haresh Ajani: 0000-0002-1223-3819

Notes

The authors declare no competing financial interest.

Acknowledgements

S.M.M.L., A.V.P. and T.M.V.D.P.eM. thank Coimbra Chemistry Centre (CQC), supported by the Portuguese Agency for Scientific Research, “Fundação para a Ciência e a Tecnologia” (FCT), through project UID/QUI/00313/2019. We also acknowledge the UC-NMR facility for obtaining the NMR data (www.nmrccc.uc.pt). C.S.B.G. acknowledges the Associate

Laboratory for Green Chemistry-LAQV which is financed by national funds from FCT/MCTES (UID/QUI/50006/2019). The authors (RJ, EŘ) wish to acknowledge the support from the European Regional Development Fund (Project ENOCH, No. CZ.02.1.01/0.0/0.0/16_019/0000868) and Palacký University in Olomouc (IGA_PrF_2019_013).

References

[1] N.G.R.D. Elshan, M.B. Rettig, M.E. Jung, Molecules targeting the androgen receptor (AR) signaling axis beyond the AR-Ligand binding domain, Med. Res. Rev. 39 (2019) 910-960.

[2] C. Bobach, S. Tennstedt, K. Palberg, A. Denkert, W. Brandt, M.A. de, B. Seliger, L.A. Wessjohann, Screening of synthetic and natural product databases: Identification of novel androgens and antiandrogens, Eur. J Med. Chem. 90 (2015) 267-279.

[3] F. Cortes-Benitez, M. Cabeza, M.T. Ramirez-Apan, B. Alvarez-Manrique, E. Bratoeff, Synthesis of 17beta-N-arylcarbamoylandrost-4-en-3-one derivatives and their anti-proliferative effect on human androgen-sensitive LNCaP cell line, Eur. J Med. Chem. 121 (2016) 737-746.

[4] C. Ferroni, A. Pepe, Y.S. Kim, S. Lee, A. Guerrini, M.D. Parenti, A. Tesei, A. Zamagni, M. Cortesi, N. Zaffaroni, C.M. De, G.L. Beretta, J.B. Trepel, S.V. Malhotra, G. Varchi, 1,4-Substituted Triazoles as Nonsteroidal Anti-Androgens for Prostate Cancer Treatment, J Med. Chem. 60 (2017) 3082-3093.

[5] Y.K. Shi, B. Wang, X.L. Shi, Y.D. Zhao, B. Yu, H.M. Liu, Synthesis and biological evaluation of new steroidal pyridines as potential anti-prostate cancer agents, Eur. J Med. Chem. 145 (2018) 11-22.

[6] D. Li, W. Zhou, J. Pang, Q. Tang, B. Zhong, C. Shen, L. Xiao, T. Hou, A magic drug target: Androgen receptor, Med. Res. Rev.(2018)

[7] D.A. Bastos, E.S. Antonarakis, Galeterone for the treatment of advanced prostate cancer: the evidence to date, Drug Des Devel. Ther. 10 (2016) 2289-2297.

[8] U.L. McClurg, M. Azizyan, D.T. Dransfield, N. Namdev, N.C.T.H. Chit, S. Nakjang, C.N. Robson, The novel anti-androgen candidate galeterone targets deubiquitinating enzymes, USP12 and USP46, to control prostate cancer growth and survival, Oncotarget. 9 (2018) 24992-25007.

[9] M. Alyamani, Z. Li, M. Berk, J. Li, J. Tang, S. Upadhyay, R.J. Auchus, N. Sharifi, Steroidogenic Metabolism of Galeterone Reveals a Diversity of Biochemical Activities, Cell Chem Biol. 24 (2017) 825-832.

[10] A. Gupta, B.S. Kumar, A.S. Negi, Current status on development of steroids as anticancer agents, J Steroid Biochem. Mol. Biol. 137 (2013) 242-270.

[11] M. Ibrahim-Ouali, Synthesis of pentacyclic steroids, Steroids. 73 (2008) 775-797.

[12] J.A. Salvador, J.F. Carvalho, M.A. Neves, S.M. Silvestre, A.J. Leitao, M.M. Silva, Sa e Melo ML, Anticancer steroids: linking natural and semi-synthetic compounds, Nat. Prod. Rep. 30 (2013) 324-374.

[13] I.V. Zavarzin, V.V. Chertkova, I.S. Levina, E.I. Chernoburova, Steroids fused to heterocycles at positions 16, 17 of the D-ring, Russ. Chem. Rev. 80 (2011) 661-682.

[14] P. Chowdhury, J.M. Borah, M. Bordoloi, P.K. Goswami, A. Goswami, N.C. Barua, P.G. Rao, A simple efficient process for the synthesis of 16-dehydropregnenolone acetate (16-DPA) - a key steroid drug intermediate from diosgenin, Chem Eng Process Technol. 2 (2011) 117.

[15] M. Kumar, P. Rawat, M.F. Khan, A.K. Rawat, A.K. Srivastava, R. Maurya, Aza-annulation on the 16-dehydropregnenolone, via tandem intermolecular aldol process and intramolecular Michael addition, Bioorg. Med. Chem Lett. 21 (2011) 2232-2237.

[16] S.M. Lopes, C.F. Correia, S.C. Nunes, N.A. Pereira, A.R. Ferreira, E.P. Sousa, C.S. Gomes, J.A. Salvador, A.A. Pais, Pinho e Melo TM, Synthesis of chiral hexacyclic steroids via [8pi + 2pi] cycloaddition of diazafulvenium methides, Org Biomol. Chem. 13 (2015) 9127-9139.

[17] S.M.M. Lopes, E.P. Sousa, L. Barreira, C. Marques, M.J. Rodrigues, Pinho E Melo TMVD, Synthesis and anti-cancer activity of chiral tetrahydropyrazolo[1,5-a]pyridine-fused steroids, Steroids. 122 (2017) 16-23.

[18] S.M.M. Lopes, C.S.B. Gomes, Pinho E Melo TMVD, Reactivity of Steroidal 1-Azadienes toward Carbonyl Compounds under Enamine Catalysis: Chiral Penta- and Hexacyclic Steroids, Org Lett. 20 (2018) 4332-4336.

[19] F.H. Allen, The Cambridge Structural Database: a quarter of a million crystal structures and rising, Acta Crystallogr. B. 58 (2002) 380-388.

[20] A.K. Kwegyir-Afful, R.D. Bruno, P. Purushottamachar, F.N. Murigi, V.C. Njar, Galeterone and VNPT55 disrupt Mnk-eIF4E to inhibit prostate cancer cell migration and invasion, FEBS J. 283 (2016) 3898-3918.

[21] D.J. McCarty, W. Huang, M.A. Kane, P. Purushottamachar, L.K. Gediya, V.C.O. Njar, Novel galeterone analogs act independently of AR and AR-V7 for the activation of the unfolded protein response and induction of apoptosis in the CWR22Rv1 prostate cancer cell model, Oncotarget. 8 (2017) 88501-88516.

[22] I. Bartonkova, A. Novotna, Z. Dvorak, Novel stably transfected human reporter cell line AIZ-AR as a tool for an assessment of human androgen receptor transcriptional activity, PLoS. One. 10 (2015) e0121316.

[23] A. Padmanabhan, V. Rao, A.M. De Marzo, C.J. Bieberich, Regulating NKX3.1 stability and function: Post-translational modifications and structural determinants, Prostate. 76 (2016) 523-533.

[24] H. Ajani, J. Jansa, C. Kopruluoglu, P. Hobza, V. Krystof, A. Lycka, M. Lepsik, Imidazo[1,2-c]pyrimidin-5(6H)-one as a novel core of cyclin-dependent kinase 2 inhibitors: Synthesis, activity measurement, docking, and quantum mechanical scoring, J Mol. Recognit. 31 (2018) e2720.

[25] R.A. Friesner, J.L. Banks, R.B. Murphy, T.A. Halgren, J.J. Klicic, D.T. Mainz, M.P. Repasky, E.H. Knoll, M. Shelley, J.K. Perry, D.E. Shaw, P. Francis, P.S. Shenkin, Glide: a new approach for rapid, accurate docking and scoring. 1. Method and assessment of docking accuracy, J Med. Chem. 47 (2004) 1739-1749.

[26] E. Gianti, R.J. Zauhar, Modeling androgen receptor flexibility: a binding mode hypothesis of CYP17 inhibitors/antiandrogens for prostate cancer therapy, J Chem Inf. Model. 52 (2012) 2670-2683.

[27] Sheldrick GM. SHELX97 - programs for crystal structure analysis (release 97-2). Institüt für Anorganische Chemie der Universität, Tammanstrasse 4, D-3400 Göttingen, Germany 1998;

[28] G.M. Sheldrick, A short history of SHELX, Acta Crystallogr. A. 64 (2008) 112-122.

[29] L.J. Farrugia, WinGX and ORTEP for Windows: an update, J. Appl. Cryst. 45 (2012) 849-854.

[30] Glide, Schrödinger, LLC, New York, NY, 2016. 2016;

[31] Schrödinger Release 2018-2: Schrödinger Suite 2018-2 Induced Fit Docking protocol. 2018;

[32] Prime, Schrödinger, LLC, New York, NY, 2018. 2018;

[33] G. Nemethy, K.D. Gibson, K.A. Palmer, Ch.N. Yoon, G. Paterlini, A. Zagari, S. Rumsey, H.A. Scheraga, Energy parameters in polypeptides. 10. Improved geometrical parameters

and nonbonded interactions for use in the ECEPP/3 algorithm, with application to proline-containing peptides, J. Phys. Chem. 96 (1992) 6472-6484.

[34] K. Kinoshita, H. Nakamura, Identification of the ligand binding sites on the molecular surface of proteins, Protein Sci. 14 (2005) 711-718.